ASME Journal of Solar Energy Engineering
Online journal at:
https://asmedigitalcollection.asme.org/solarenergyengineering

Experimental Performance of a Nonlinear Control Strategy to Regulate Temperature of a High-Temperature Solar Reactor

Assaad Alsahlani
Engineering Technical College,
Al-Furat Al-Awsat Technical University,
Al-Najaf 54001, Iraq
e-mail: assaad.alsahlani.cnj@atu.edu.iq

Nesrin Ozalp[1]
Fellow ASME
Mechanical and Civil Engineering Department,
Purdue University Northwest,
Hammond, IN 46323
e-mail: nozalp@pnw.edu

Despite the significant potential of solar thermochemical process technology for storing solar energy as solid-state solar fuel, several challenges have made its industrial application difficult. It is important to note that solar energy has a transient nature that causes instability and reduces process efficiency. Therefore, it is crucial to implement a robust control system to regulate the process temperature and tackle the shortage of incoming solar energy during cloudy weather. In our previous works, different model-based control strategies were developed namely a proportional integral derivative controller (PID) with gain scheduling and adaptive model predictive control (MPC). These methods were tested numerically to regulate the temperature inside a high-temperature tubular solar reactor. In this work, the proposed control strategies were experimentally tested under various operation conditions. The controllers were challenged to track different setpoints (500 °C, 1000 °C, and 1450 °C) with different amounts of gas/particle flowrates. Additionally, the flow controller was tested to regulate the reactor temperature under a cloudy weather scenario. The ultimate goal was to produce 5 kg of reduced solar fuel magnesium manganese oxide ($MgMn_2O_4$) successfully, and the controllers were able to track the required process temperature and reject disturbances despite the system's strong nonlinearity. The experimental results showed a maximum error in the temperature setpoint of less than 0.5% (6 °C), and the MPC controller demonstrated superior performance in reducing the control effort and rejecting disturbances. [DOI: 10.1115/1.4062483]

Keywords: solar energy, solar fuel, MPC, thermal storage, heat transfer, solar receiver

1 Introduction

Solar fuels are energy carriers in which solar energy can be converted into a storable and transportable form. Utilizing concentrated solar energy allows for the production of solar fuel since the solar energy is stored by the reactants through thermochemical endothermic processes. A number of studies have been conducted to investigate various thermochemical energy storage candidates. However, the utilization of thermochemical energy storage system is constrained by the charging/discharging temperature range, volumetric energy, and the number of reuse cycles (lifetime) [1]. The charge/discharge temperature range in thermochemical energy storage systems depends on the chemical nature of the reactant used. For instance, the temperature range for the dehydration of metal hydroxides is 250–800 °C, whereas the temperature range is 100–950 °C for the decarboxylation of metal carbonates [2]. At higher temperatures, $MgMn_2O_4$ reacts between 1000 °C and 1500 °C [3].

Solar reactors are utilized for the thermochemical storage of solar energy, where concentrated solar energy is used to directly transfer heat to reactants through a window or indirectly transferred using a windowless reactor. The selection of a suitable solar reactor type is crucial in ensuring an effective chemical conversion process in a solar-driven high-temperature thermochemical reaction system. While window-type solar reactors are commonly used for low temperatures [4], a windowless plug-flow tubular solar reactor is preferred for high-temperature thermochemical reactions due to the melting point of reactor window components. In this type of reactor, the reactants are heated as a result of direct concentrated solar flux irradiation of the reactor tube wall, which is contained within a receiver cavity. In plug-flow tubular solar reactors, the chemical conversion process requires a flowing gas through the reactor tube and a steady-state activation temperature to ensure an efficient conversion process.

Maintaining a quasi-temperature within the reactor during on-sun operation is challenging due to the transitory nature of solar energy. Therefore, it is necessary to develop an effective control system to regulate the temperature consistently. To design an effective control system, it is essential to pre-evaluate the control system through a numerical model to reduce effort, time, and cost. The numerical analysis of a solar reactor, including flowing media and complex heat transfer modes, is not straightforward. However, a simplified numerical model is preferable for control purposes.

[1]Corresponding author.

Contributed by the Solar Energy Division of ASME for publication in the Journal of Solar Energy Engineering: Including Wind Energy and Building Energy Conservation. Manuscript received March 15, 2023; final manuscript received April 26, 2023; published online May 19, 2023. Assoc. Editor: S.A. Sherif.

Indirectly heated packed-bed reactors are numerically analyzed using the finite volume method [5,6], while moving beds in tubular solar reactors are modeled as tubes exposed to an external heat flow with more complicated parameters [7]. The heat transfer interaction between granular flows was the basis for the thermal analysis of gravity-driven granular flow [8]. Recently, Huang et al. [9] developed a computational fluid dynamics (CFD) model to characterize the thermal properties of a 1D model plug-flow tubular reactor used for thermochemical energy storage system with counter-current flowing pellet-gas. The analysis of the 1D model was further extended to analyze 2D numerical model for the same system, where the numerical accuracy was enhanced compared to the 1D model [10]. In general, a thorough 2D or 3D CFD models are required to simulate two-phase flow problems to the acceptable level of accuracy.

The temperature inside the solar reactor can be controlled by adjusting the incoming direct normal irradiance (DNI) received by the reactor, or by adjusting the flowrates of gas/reactants. Using a variable size aperture to adjust the incoming DNI has proven to be an effective approach in cavity-type solar receivers [11]. Aiming the heliostats is another method to adjust the DNI by implementing a conventional proportional integral derivative (PID) controller, where the reactor temperature can be regulated [12]. Using model-based feedforward, the performance of the PID controller can be enhanced to control the temperature effectively in solar direct steam generation [13]. A simple form of proportional integral (PI) controller has also been implemented to regulate the temperature of a packed-bed tubular solar reactor [14].

Manipulating the gas flow is another approach to regulating the temperature in steam gasification of petcoke and carbothermal reduction [11]. Nevertheless, more advanced control methodologies, such as model predictive control (MPC) strategy, are preferred for systems with high nonlinearity, such as thermochemical reaction kinetics. This is because the production of solar fuel is a complicated dynamic process that involves multiple variables, including gas flow, solar fuel mass flowrate, and solar flux. Although the MPC controller has been shown to be a successful method for controlling the temperature of solar reactors, it involves more computational effort and optimization than a linear traditional PID controller [15].

In our previous works, we investigated the dynamics of a plug-flow tubular solar reactor used to produce $MgMn_2O_4$ solar fuel. Our earlier work [16] focused on developing a simplified physical model that was used to predict the temperature distribution along a horizontal tube solar reactor during the heating and cooling processes. The results from the numerical code demonstrated reasonable accuracy in the prediction of thermal performance for different operation conditions. The results from the low-order physical model were then used to design a PI control system to regulate the temperature inside a horizontal tube with packed bed [14]. The numerical analysis was extended to include a more complicated heat transfer model to study the dynamics of a high-temperature vertical tubular reactor with counter-current flowing pellet-gas. The system consists of a vertically oriented tubular reactor surrounded by heating elements at one segment, with the $MgMn_2O_4$ pellets fed from the top end through a funnel, and the gas was supplied from the bottom end. The sensible heat of the downward-moving pellets is recovered by a counter-current air flow, resulting in gas and pellets entering and leaving the reactor tube at temperatures close to room temperature. The inhouse code was tested under different operating conditions, including different particle/gas mass flowrates and heating levels. The numerical results showed excellent agreement between simulated and experimental data [17].

The low-order physical model was implemented to design a model-based combined PID controller, which was numerically tested to track different setpoints by simulating various weather conditions [15]. In our recent work [18], we used the inhouse code to evaluate another model-based control strategy, including an adaptive model predictive controller, to control the temperature inside a tubular plug-flow solar reactor. The results from the numerical code were used to improve the controller's performance by incorporating an updated algorithm to estimate controlling states via a system identification procedure. The performance of the proposed adaptive MPC was simulated to track different temperature setpoints and different operating conditions, including the chemical reaction at high temperatures.

In this work, the numerical control models presented in Refs. [17,18] were experimentally validated for the same vertical tubular reactor with different heating levels and particle/gas mass flowrates. The PID and MPC controllers were tested to track a steady-state setpoint of 1450 °C during the production of 5 kg of reduced solar fuel $MgMn_2O_4$ particles. The PID control system utilized a gain scheduling approach to model the system nonlinearity, while the MPC controller utilized a system identification process to estimate the measured temperature online by incorporating adaptive loop within the numerical code. The experimental methodology is presented in Sec. 2, the design of control systems is presented in Sec. 3, and the experimental results discussed in Sec. 4.

2 Experimental Setup

This research includes experimental testing to evaluate the performance of nonlinear control strategies used for regulating the temperature inside a solar reactor that features counter-current flowing gas and solid particles. The solar reactor is utilized in the production of a solid-state solar fuel $MgMn_2O_4$ by heating the reactor up to 1500 °C.

The thermal characteristics of the reactor were thoroughly studied in our previous works [14,16] by validating a simplified 1D heat transfer model under different operating conditions. The temperature inside the solar reactor can be controlled by adjusting the incoming solar power or the flowrate of the fluid/gas passing through the reactor. Numerical models of PID and MPC were successfully tested in our recent works [17,18]. The experimental setup consists of a reactor unit, control system, data acquisition (DAQ), and power supply unit. The reactor consists of a 152.4 cm in length alumina tube centered vertically through a 30.5 cm heating zone.

The reactor tube is heated circumferentially via a heat flux controlled by an adjustable power supply. The reactor tube receives $MgMn_2O_4$ particles of 3–3.66 mm in size from a funnel mounted at the top end of the tube. A gas-pulsation valve mechanism is installed at the bottom end of the reactor tube to control the particle's mass flowrate, and the discharged particles were collected inside a tank beneath the setup. The gas flowrate is controlled by a digital Alicat gas flow controller, with the gas flows in a counter-current orientation from bottom to top.

The counter-current flowing gas is utilized to recuperate the sensible heat of the downward flowing pellets using ($c_{p_s}\dot{m}_s = c_{p_g}\dot{m}_g$). A B-type thermocouple is installed at the center of the heating zone, and the measured temperature is received by DAQ USB-6343 from National Instruments to be analyzed by the control model deployed on LABVIEW software by NI™. The output from the control system is fed to an silicon controlled rectifiers (SCR) power supply unit through the DAQ. The SCR power supply unit receives a signal of 4–20 mA whereas, the DAQ unit provides a voltage signal of 0–5 V. Therefore, a voltage-to-current converter module is used to link the DAQ output to a digital SCR input. Since the heat recuperation condition was considered, the amount of gas and particles mass flowrates are interrelated to maintain this condition. Hence, the signal provided from the DAQ to the flow controllers can be split via a proportional constant K, as shown in Fig. 1(*a*).

3 Design of the Control Systems

3.1 Design of the Proportional Integral Derivative Controller. A conventional PID controller is implemented since it is the most commonly used control method in the industry. The control action, Δu, is defined by the discrete-time form of the

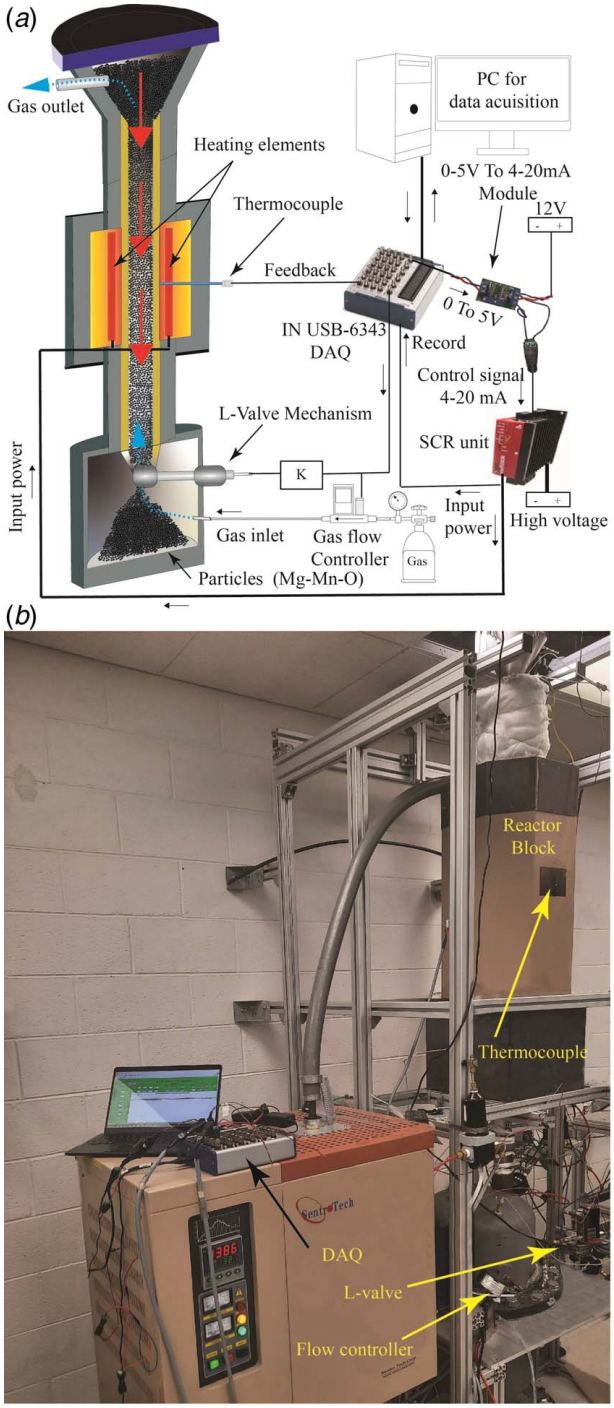

Fig. 1 Experimental setup: (*a*) schematic diagram and (*b*) photo of the setup

PID controller, as follows:

$$\Delta u(t_k) = \left(K_P + \frac{K_P \Delta t}{\tau_I} + \frac{K_P \tau_D}{\Delta t}\right) e(t_k) - \left(K_P + \frac{2K_P \tau_D}{\Delta t}\right) e(t_{k-1}) + \frac{K_P \tau_D}{\Delta t} e(t_{k-2}) \quad (1)$$

where K_P, τ_D, and τ_I are the controller parameters to be tuned using the Ziegler–Nichols method. $e(t_k)$ is the error between the measured output and its setpoint at the sampling time t_k, and Δt is the sampling time interval.

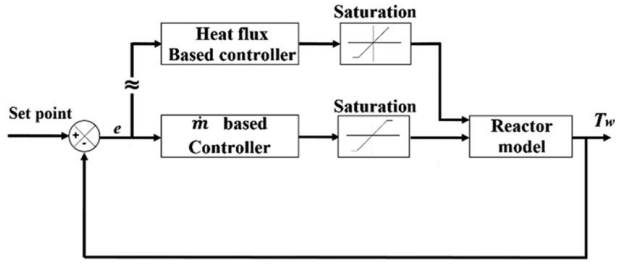

Fig. 2 Control system loop to regulate reactor temperature at the heating zone

The control system consists of two controllers: A controller to regulate the input heat flux, whereas the other controller adjusts the particles mass flowrate, as shown in Fig. 2. To maintain the heat recuperation condition, mass flowrates of the gas and particles are interrelated, which technically requires one controller. The flow controller is an incremental controller with a fixed value of mass flow increment, and it is to be activated when the heat flux controller is saturated or fails to track the desired setpoint due to insufficient input power.

3.2 Design of the Model Predictive Control Controller. MPC is a widely used optimization control method in industry due to its excellent control effects and robustness. Unlike classical control methods, such as PID control, MPC can optimize the system while it is operating and handle nonlinear processes (MIMO) by accounting for constraints of the system [19]. The main concept in developing an MPC control strategy is to use system models to predict future outputs within number of time-steps known as the prediction horizon, N_p, incorporating different corresponding control actions over set of time-steps known as the control horizon, N_u. Additionally, MPC can optimize the response by generating future control signals that closely match the process output and the reference trajectory, utilizing known input from the past. By updating the system model during the process, MPC can model system nonlinearity online, as shown in Fig. 3. Our previous work validated the temperature control in the solar reactor through numerical simulations using adaptive model predictive control [16], and we conducted experimental evaluations of the proposed control scheme in the present study. To implement the control scheme, a generalized predictive controller (GPC) based on an autoregressive with extra input (ARX) model of a linearized solar reactor was utilized [20]

$$A(q^{-1}) = B(q^{-1})u(k-1) + e(k) \quad (2)$$

$$A(q^{-1}) = 1 + a_1 q^{-1} + a_2 q^{-2} + \cdots + a_{na} q^{-na} \quad (3)$$

$$B(q^{-1}) = b_0 + b_1 q^{-1} + b_2 q^{-2} + \cdots + b_{nb} q^{-nb} \quad (4)$$

where $y(k)$ represents the output of the process (°C), $u(k)$ represents the control input (heat flux) variable at sampling time k, $A(q^{-1})$ and $B(q^{-1})$ represent the model polynomial matrices, $e(k)$ is a white noise (assumed to be negligible in this work), and q^{-1} is the backward shift operator.

In order to identify the model parameters a_1 and b_1, a recursive least squares method with a forgetting factor is used as follows [20]:

$$\hat{y}(k) = \varphi^T(k)\,\hat{\theta}(k-1) \quad (5)$$

where φ^T is the column vector of the past inputs and output values which is defined as

$$\varphi^T(k) = [y(k-1), y(k-2), y(k-3), u(k), u(k-1), u(k-2), u(k-3)] \quad (6)$$

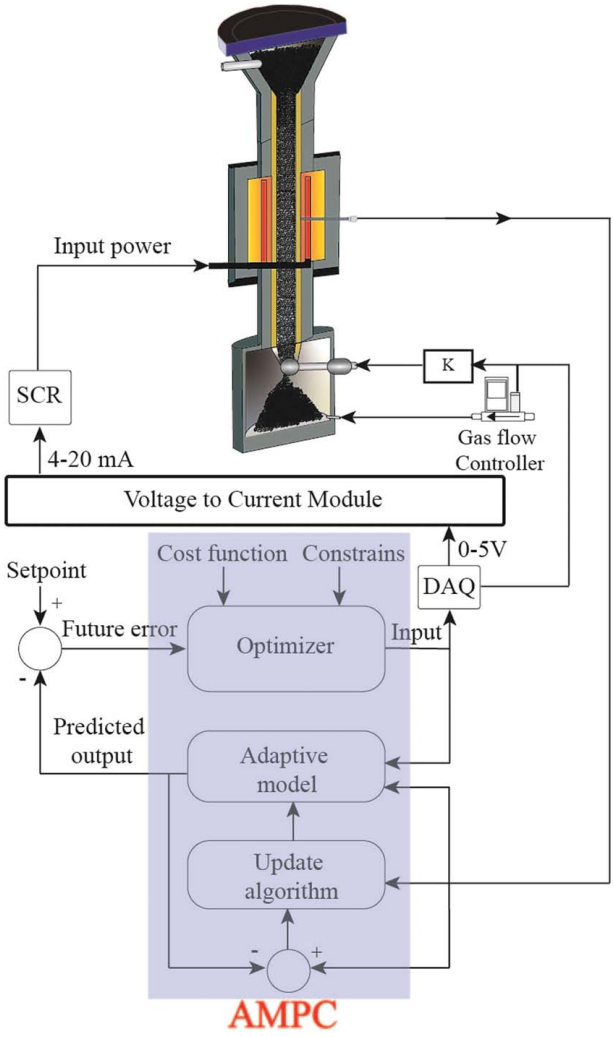

Fig. 3 Feedback control diagram for adaptive MPC controller

where $\hat{\theta}$ is the estimation of model parameters which is defined as

$$\hat{\theta}(k) = [a_1, a_2, a_3, b_o, b_1, b_2, b_3] \tag{7}$$

and calculated by using

$$\hat{\theta}(k) = \hat{\theta}(k-1) + \frac{P(k-1)\varphi(k)}{\lambda(k) + \varphi^T(k)\,P(k-1)\varphi(k)}(y(k) - \hat{y}(k)) \tag{8}$$

where $P(k)$ represents the covariance matrix of estimation errors which is defined as

$$P(k) = \frac{1}{\lambda(k)}\left[P(k-1) - \frac{P(k-1)\varphi(k)\varphi^T(k)P(k-1)}{\lambda(k) + \varphi^T(k)\,P(k-1)\varphi(k)}\right] \tag{9}$$

where $\lambda(k)$ is the forgetting factor which is calculated from

$$\lambda(k) = \max\left[\left(1 - \frac{y(k) - \hat{y}(k)}{1 + (y(k) - \hat{y}(k))^2}\right), \lambda_{\min}\right] \tag{10}$$

The estimated ARX model was then used to optimize the control action of the system by implementing the GPC algorithm, which minimizes the cost function J defined as [18]

$$J(N_p, N_u) \sum_{j=1}^{N_p} [\hat{y}(k+j|k) - w(k+j)]^2 + \sum_{j=1}^{N_u} \omega_j[\Delta u(k+j-1|k)]^2 \tag{11}$$

where $\hat{y}(k+j|k)$ is ahead output prediction at time interval k, and $w(k+j)$ is the future reference trajectory, which is defined as the desired setpoint. ω_j is the weighing parameter, which is to be adjusted properly to follow the reference trajectory. The MPC controller needs to be tuned in a manner similar to tuning the PID controller. The parameters to be tuned are N_p, N_u, and ω values.

4 Experimental Results

The experiment tests included the tuning processes and final testing of both PID and MPC controllers as follows:

4.1 Proportional Integral Derivative Controller. First, the PID controller's parameters were tuned experimentally by heating the system with a packed bed from room temperature to 800 °C with a heating rate of 5.5 °C/min and a sampling time of 1 s. At the beginning of the heating process, the response temperature error fluctuated, and the tuning process was challenging due to the thermal inertia (transient) of the reactor block. However, the response tended to stabilize, and the controller accurately tracked the desired setpoint until the end of the test, as shown in Fig. 4(*a*). The controller parameters were obtained as $K_P = 0.87$, $K_I = 0.0076$, and $K_D = 2.1 \times 10^{-6}$. Although the temperature response was relatively smooth when the suitable controller parameters were specified (when $T > 400$ °C), the control input was relatively aggressive and severely fluctuated during the heating process, as depicted in Fig. 4(*b*). This was attributed to the limited response of the PID and the computational effort due to the value of the sampling time where the response of the SCR power supply alternates within high voltage range leading to significant fluctuates in power supply and hence temperature output fluctuates as well. One more test was performed to ensure the readiness of the PID controller and observe the possibility of using a smaller sampling time as shown in Fig. 5.

The controller was tested to track different setpoints including steady-state at 400 °C, heating up to 500 °C, and cooling down to 400 °C, as shown in Fig. 5, with a sampling time of 0.5 s. It can be noticed that the control system tracked the desired setpoints reasonably, and the input signal is less aggressive when compared to the process with a sampling time of 1 s (Fig. 4). Therefore, minimizing the sampling time is the key to obtaining a smoother response and less control effort.

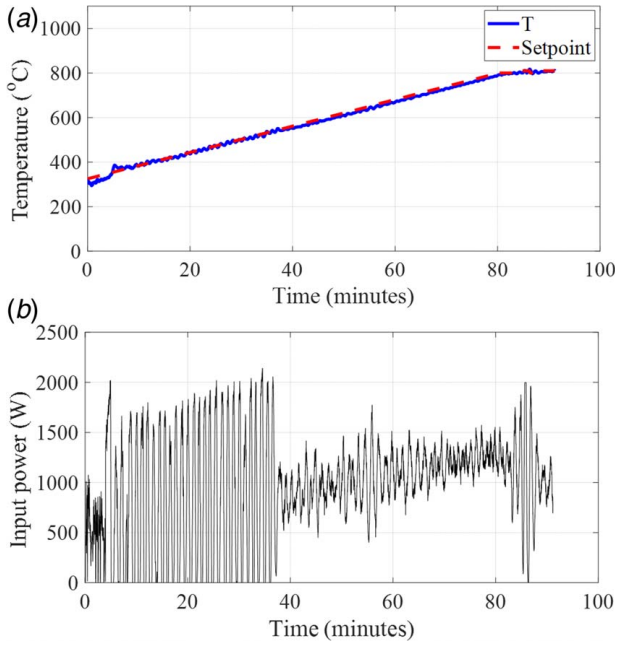

Fig. 4 The system response obtained from the PID controller during and after tuning process with 1 s sampling time

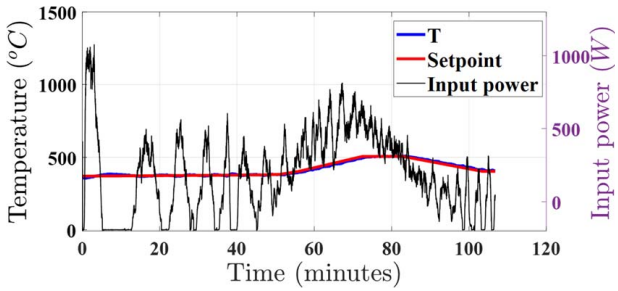

Fig. 5 Results from PID controller to track different setpoints with sampling time of 0.5 s

It was noticed that the PID controller operates accurately with a slight change in the values of controller parameters depending on the operating condition. This is expected, as the reactor system involves inherent nonlinearities resulting from temperatures with higher order in addition to the nonlinearity from reaction kinetics, in addition to the strong nonlinearity associated with the thermochemical reaction of $MgMn_2O_4$. Therefore, it is practically suitable to implement gain scheduling technique with gain values close to the ones obtained from experimental tuning. With that said, the PID controller was challenged to regulate the temperature inside the reactor over a period of 3 h, including 90 min, which is enough to produce more than 5 kg of the solar fuel (charged particles).

Figure 6 illustrates the temperature response and corresponding input power during the production of solar fuel. The system was heated from room temperature to 1000 °C with a packed bed. Thereafter, the flow of gas/particles was initiated with a particle mass flowrate of 1.25 g/s and gas flowrate of 60 SLPM (Nitrogen). Meanwhile, the system was continuously heated up to 1450 °C with a heating rate of 4.5 °C/min and held steady for 80 min. The PID controller closely tracked the desired setpoint and handled the system nonlinearity in the presence of the thermochemical reaction, with small steady-state error and reasonable overshoot. Also, the large variations in the input power were significantly reduced by decreasing the sampling time to 50 ms, indicating a quick controller response.

4.2 Model Predictive Control Controller. The MPC controller was experimentally tuned and tested to track setpoints similar to those used in testing the PID controller. The MPC utilizes a system

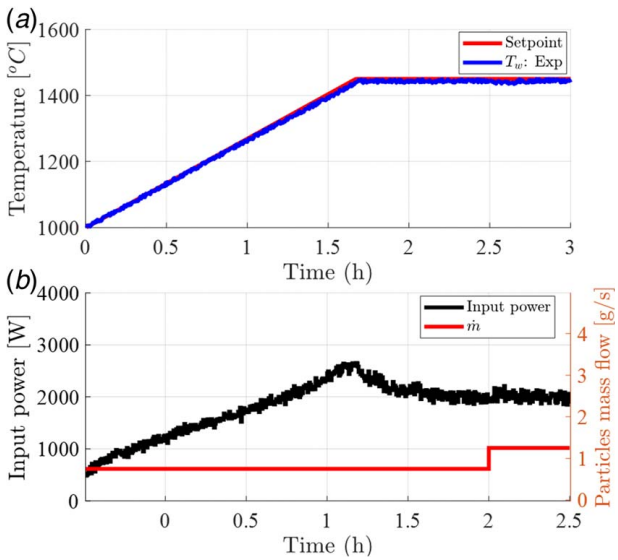

Fig. 6 Final test of the PID controller during the production process of the solar fuel

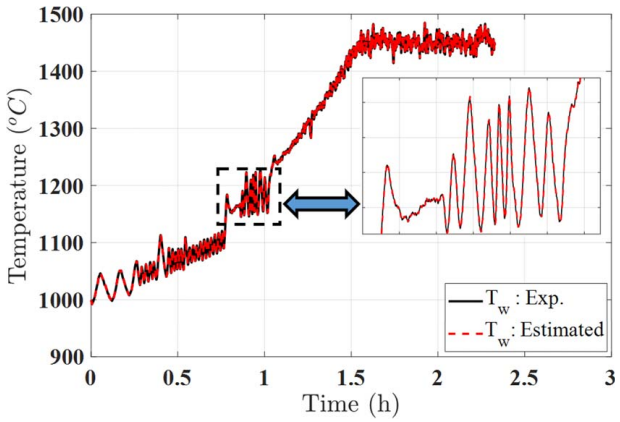

Fig. 7 Results from system identification algorithm used for the MPC

identification block coded within the MPC loop to estimate the system states online during the control process. Figure 7 illustrates a comparison between the experimentally measured temperature and the estimated temperature obtained by the system identification algorithm as shown in the magnified subplot. Despite the inconsistent and strongly fluctuating nature of the measured temperature, the numerically estimated temperature is very accurate and almost identical to the measured temperature, accurately simulating its behavior over time.

The final test of the MPC controller involved tuning the MPC parameters N_p, N_u, and ω to minimize the cost function in Eq. (11) and the results are illustrated in Fig. 8. The results showed that the optimal control action was achieved when $N_p = 103$, $N_u = 100$, and $\omega = 82$. Similar to the PID controller, the MPC was challenged to regulate the temperature inside the reactor during the production of the solar fuel with a sampling time of 50 ms, and 0.75 g/s particle flowrate, and 36 SLPM gas flowrate. The controller tracked the desired setpoint (1450 °C) successfully and handled the system nonlinearity during the thermochemical reaction. Moreover, the overshoot in the measured temperature is 15% for the MPC, which is less than the overshoot observed in the PID controller (25%). The robustness of the MPC controller was also tested by suddenly increasing the particle's mass flowrate to 1 g/s during the steady-state, causing a sudden drop in temperature. The MPC increased the input power accordingly and brought the temperature

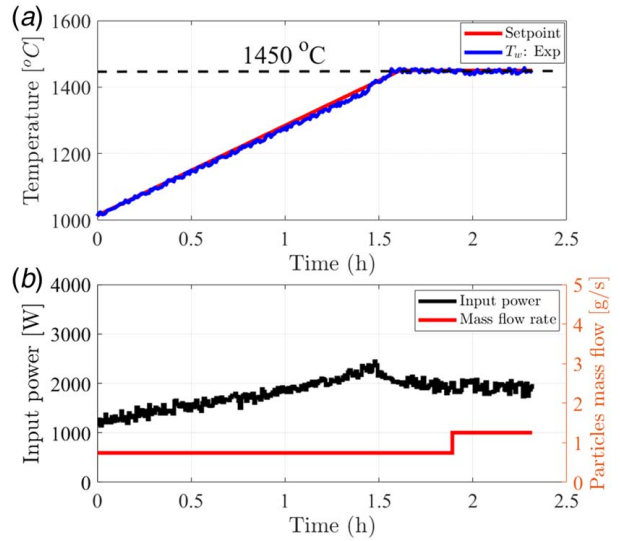

Fig. 8 The performance of the MPC controller during different operating conditions with sampling time of 50 ms

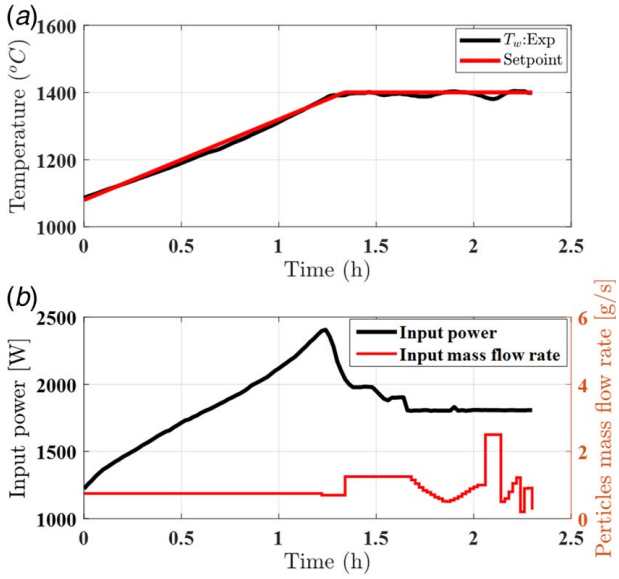

Fig. 9 Performance of the flow controller under different operating conditions

back to the setpoint (1450 °C). The measured temperature for the MPC controller tends to show high oscillations in measured temperature due to the malfunction in the thermocouple connection during the process.

The last test was conducted to evaluate the performance of the flow controller by simulating the transient nature of solar power as shown in Fig. 9. The system was heated up to 1400 °C and held steady with a particle flowrate of 1.25 g/s and corresponding input power of around 1900 W. The input power is lowered to a constant value of 1800 W, and the flow controller was initiated to reduce the mass flowrate, heating up the reactor and bringing the temperature back to the setpoint until the mass flowrate converged to 0.92 g/s and the temperature was close to 1400 °C. To further test the flow controller, it was switched off, and the mass flowrate was increased to 2.5 g/s and maintained at that value for approximately 10 min until the temperature decreased by more than 30 °C. Once the flow controller was switched on, it began regulating the flowrate gradually until the temperature was brought back to the setpoint.

5 Conclusions

In this work, two control strategies were tested experimentally to regulate the temperature in a high-temperature tubular solar reactor that is used to produce solid-state solar fuel as a long-term thermal storage. The experimental setup consisted of a solar reactor unit housing a vertically oriented tubular reactor that is heated circumferentially via electric heaters. The inert particles are fed to the reactor tube from the top and the counter-current flowing gas is supplied to the tube from the bottom. The temperature of the reactor tube at the heating zone is measured and fed to the PC through a DAQ unit. The input signal is then analyzed numerically by control algorithms, and the control decision is fed to an SCR power supply unit to regulate the input power received by the electric heater or fed to the flow controller. First, a conventional PID controller was used with a gain scheduling method to regulate the temperature during the nonlinear process. Second, an MPC with a system identification block was used to estimate the system state online. Both control systems were tested to track ramping temperature and maintain steady-state temperature at 1450 °C to produce 5 kg of charged solar fuel. Both control strategies showed good tracking ability and quick response where the sampling time is 50 ms. The maximum steady-state error was <0.5% (6 °C) for all tests. Although both control strategies showed similar performance, the MPC had required less input power to achieve the desired output and better at handling the sudden disturbances compared to the PID. The flow controller was also tested by applying constant input power to simulate cloudy weather. The flow controller was able to regulate the temperature by adjusting the amount of particle/gas mass flowrates. The proposed control strategies showed very fast response with a small sampling time of 50 ms and can be successfully implemented in high-temperature solar applications.

Acknowledgment

This material is based upon work supported by the U.S. Department of Energy's Office of Energy Efficiency and Renewable Energy (EERE) under the Solar Energy Technology Office (SETO) Award Number DE–EE0008992. The authors would like to express great appreciation to Kelvin Randhir Michael Hayes and Philipp Schimmels for their support and collaboration in this work.

Conflict of Interest

There are no conflicts of interest.

Data Availability Statement

The authors attest that all data for this study are included in the paper.

Nomenclature

c_p = specific heat (J/kg/K)
D_i = tube inner diameter (m)
D_o = tube outside diameter (m)
N_p = prediction horizon
N_u = control horizon
Q_{in} = input power at heating zone (W)
q'' = heat flux (W/m^2)
q^{-1} = backward shift operator
n_a, n_b = polynomial orders for A and B
K_D, K_p = coefficients of the PI controller

Greek Symbol

τ_1 = coefficient of the PI controller

References

[1] Sunku Prasad, J., Muthukumar, P., Desai, F., Basu, D. N., and Rahman, M. M., 2019, "A Critical Review of High-Temperature Reversible Thermochemical Energy Storage Systems," Appl. Energy, **254**, p. 113733.
[2] Prieto, C., Cooper, P., Fernández, A. I., and Cabeza, L. F., 2016, "Review of Technology: Thermochemical Energy Storage for Concentrated Solar Power Plants," Renewable Sustainable Energy Rev., **60**, pp. 909–929.
[3] Randhir, K., King, K., Rhodes, N., Li, L., Hahn, D., Mei, R., AuYeung, N., and Klausner, J., 2019, "Magnesium-Manganese Oxides for High Temperature Thermochemical Energy Storage," J. Energy Storage, **21**, pp. 599–610.
[4] Abedini Najafabadi, H., and Ozalp, N., 2018, "Aperture Size Adjustment Using Model Based Adaptive Control Strategy to Regulate Temperature in a Solar Receiver," Sol. Energy, **159**, pp. 20–36.
[5] Abedini Najafabadi, H., and Ozalp, N., 2018, "An Advanced Modeling and Experimental Study to Improve Temperature Uniformity of a Solar Receiver," Energy, **165**, pp. 984–998.
[6] Wang, B., Li, L., Pottas, J. J., Bader, R., Kreider, P. B., Wheeler, V. M., and Lipiński, W., 2020, "Thermal Model of a Solar Thermochemical Reactor for Metal Oxide Reduction," ASME J. Sol. Energy Eng., **142**(5), p. 051002.
[7] Wyttenbach, J., Bougard, J., Descy, G., Skrylnyk, O., Courbon, E., Frère, M., and Bruyat, F., 2018, "Performances and Modelling of a Circular Moving Bed Thermochemical Reactor for Seasonal Storage," Appl. Energy, **230**, pp. 803–815.
[8] Guo, Z., Yang, J., Tan, Z., Tian, X., and Wang, Q., 2021, "Numerical Study on Gravity-Driven Granular Flow Around Tube Out-Wall: Effect of Tube Inclination on the Heat Transfer," Int. J. Heat Mass Transfer, **174**, p. 121296.

[9] Huang, W., Korba, D., Randhir, K., Petrasch, J., Klausner, J., AuYeung, N., and Li, L., 2022, "Thermochemical Reduction Modeling in a High-Temperature Moving-Bed Reactor for Energy Storage: 1D Model," Appl. Energy, **306**, p. 118009.
[10] Korba, D., Huang, W., Randhir, K., Petrasch, J., Klausner, J., AuYeung, N., and Li, L., 2022, "A Continuum Model for Heat and Mass Transfer in Moving-Bed Reactors for Thermochemical Energy Storage," Appl. Energy, **313**, p. 118842.
[11] Mészáros, A., Rusnák, A., and Fikar, M., 1999, "Adaptive Neural PID Control Case Study: Tubular Chemical Reactor," Comput. Chem. Eng., **23**, pp. S847–S850.
[12] Petrasch, J., Osch, P., and Steinfeld, A., 2009, "Dynamics and Control of Solar Thermochemical Reactors," Chem. Eng. J., **145**(3), pp. 362–370.
[13] Mokhtar, M., Zahler, C., and Stieglitz, R., 2022, "Control of Concentrated Solar Direct Steam Generation Collectors for Process Heat Applications," ASME J. Sol. Energy Eng., **144**(1), p. 011005.
[14] Alsahlani, A., Randhir, K., Ozalp, N., and Klausner, J., 2022, "A Forward Feedback Control Scheme for a Solar Thermochemical Moving Bed Counter-Current Flow Reactor," ASME J. Sol. Energy Eng., **144**(3), p. 031004.
[15] Rowe, S. C., Hischier, I., Palumbo, A. W., Chubukov, B. A., Wallace, M. A., Viger, R., Lewandowski, A., Clough, D. E., and Weimer, A. W., 2018, "Nowcasting, Predictive Control, and Feedback Control for Temperature Regulation in a Novel Hybrid Solar-Electric Reactor for Continuous Solar-Thermal Chemical Processing," Sol. Energy, **174**, pp. 474–488.
[16] Alsahlani, A., Randhir, K., Ozalp, N., and Klausner, J., 2022, "A Simplified Numerical Approach to Characterize the Thermal Response of a Moving Bed Solar Reactor," ASME J. Therm. Sci. Eng. Appl., **14**(8), p. 081010.
[17] Alsahlani, A., Randhir, K., Hayes, M., Schimmels, P., Ozalp, N., and Klausner, J., 2023, "Design of a Combined PID Controller to Regulate the Temperature Inside a High-Temperature Tubular Solar Reactor," ASME J. Sol Energy Eng., **145**(1), p. 011011.
[18] Alsahlani, A., Randhir, K., Hayes, M., Schimmels, P., Ozalp, N., and Klausner, J., 2023, "Implementation of a Model Predictive Control Strategy to Regulate Temperature Inside Plug-Flow Solar Reactor With Counter-Current Flow," ASME J. Thermal Sci. Eng. Appl., **15**(2), p. 021013.
[19] Abedini Najafabadi, H., Ozalp, N., Ophoff, C., and Moens, D., 2019, "An Experimental Study on Temperature Control of a Solar Receiver Under Transient Solar Load," Sol. Energy, **186**, pp. 52–59.
[20] Abuseada, M., and Ozalp, N., 2020, "Experimental and Numerical Study on a Novel Energy Efficient Variable Aperture Mechanism for a Solar Receiver," Sol. Energy, **197**, pp. 396–410.